

# Directed, Elliptic and Triangular Flows in Asymmetric Heavy Ion Collisions

M. Bleicher<sup>1,3</sup>, K. A. Bugaev<sup>2</sup>, P. Rau<sup>1,3</sup>, A. S. Sorin<sup>4</sup>, J. Steinheimer<sup>1,3</sup>, and H. Stöcker<sup>1,5</sup>

<sup>1</sup>Frankfurt Institute for Advanced Studies (FIAS), 60438 Frankfurt, Germany

<sup>2</sup>Bogolyubov Institute for Theoretical Physics, National Academy of Sciences of Ukraine, 03680 Kiev, Ukraine

<sup>3</sup>Institut für Theoretische Physik, Goethe-Universität, 60438 Frankfurt, Germany

<sup>4</sup>Joint Institute for Nuclear Research (JINR), 141980 Dubna, Moscow Region, Russia

<sup>5</sup>GSI Helmholtzzentrum für Schwerionenforschung, 64291 Darmstadt, Germany

emails: bleicher@th.physik.uni-frankfurt.de bugaev@th.physik.uni-frankfurt.de  
rau@th.physik.uni-frankfurt.de sorin@theor.jinr.ru steinheimer@th.physik.uni-frankfurt.de  
h.stoecker@gsi.de

## Abstract

In this paper we propose to thoroughly investigate asymmetric nuclear collisions both in the fixed target mode at the laboratory energy below 5 GeV per nucleon and in the collider mode with a center of mass energy below 11 GeV per nucleon. Using the UrQMD transport model, we demonstrate a strong enhancement of directed and elliptic flow coefficients for the midcentral asymmetric nuclear collisions compared to symmetric collisions. We argue that such an enhancement is due to the disappearance of the nuclear shadowing effect on the side of the smaller projectile nucleus. An analysis of the energy and centrality dependencies of the directed, elliptic and triangular flows at midrapidity shows us their sensitivity to the details of the employed model of hadronic interaction. In general, the flow patterns found for asymmetric nuclear collisions have a very rich and complicated structure of energy and centrality dependencies compared to the flows found for symmetric collisions and are worth to be investigated experimentally. The directed, elliptic, and triangular flow coefficients are computed for target nuclei containing high density fluctuations and thoroughly compared with that ones obtained in the absence of such fluctuations.

**Keywords:** asymmetric nuclear collisions, directed flow, elliptic flow, triangular flow

**PACS:** 25.75.Nq, 25.75.-q

**1. Introduction.** The experimental study of strongly interacting matter has reached a decisive moment: it is hoped that the low energy heavy ion collisions programs performed at the CERN SPS and the BNL RHIC and two new programs that are planned to begin in a few years at NICA (JINR, Dubna) and FAIR (GSI, Darmstadt) will allow the heavy ion community to locate the mixed phase of the deconfinement phase transition and to discover a possible (tri)critical endpoint. The major experimental information [1, 2, 3, 4, 5] is provided

by the measurements of particle yields, one particle momentum spectra, two particle correlations, and the Fourier components of the collective hadronic flow [6] known as  $v_1$ -coefficient (directed flow),  $v_2$ -coefficient (elliptic flow), and  $v_3$ -coefficient (triangular flow). Although the great success of experiments at the BNL RHIC [1, 2] and at the CERN LHC [3, 4, 5] proved the high efficiency of modern experimental methods, their results also clearly demonstrated that the heavy ion collisions programs at RHIC, SPS, NICA and FAIR energy range are not simpler and they require further development of both new experimental approaches and far more sophisticated theoretical models in order to reach their goals. Therefore, in view of new opportunities opening with the Nuclotron program Baryonic Matter@Nuclotron (BMN) [7, 8] which will start at JINR (Dubna) in 2014, we would like to address here some new physical issues that can be studied at laboratory energies of 2 – 5 AGeV for a wide range of colliding nuclei in the fixed target mode. In future, they can also be further investigated at the accelerators of new generation like NICA (JINR, Dubna) and FAIR (GSI, Darmstadt) at a center of mass energy up to 11 AGeV.

This range of energies was thoroughly investigated in the past at the GSI SIS and the BNL AGS experiments, but only for symmetric nuclear collisions A+A. In this paper we demonstrate by using the Ultrarelativistic Quantum Molecular Dynamics transport model UrQMD [9, 10] that one of the major tasks of the low energy programs at JINR and GSI could be a systematic study of directed, elliptic, and triangular flows for non-central asymmetric nuclear collisions (ANC), i.e. for non-central  $A + B$  reactions with  $1 \ll B \ll A$  (see Fig. 1). This aspect of heavy ion physics was not yet systematically explored. Until today there were only a few works reported for ANC [11, 12, 13]. Moreover, these works were completed before a systematic investigation of the Fourier components [6] of hadronic flow was proposed. Therefore, here we argue that at lab. energies of about 2 – 10 AGeV a systematic study of  $v_1$ ,  $v_2$  and  $v_3$  Fourier-coefficients of the azimuthal particle distributions measured in non-central ANC with a special choice of impact parameter may help to essentially improve our understanding of the hadronic matter equation of state at high densities. In addition, under certain conditions, highest baryonic charge densities can be reached in these experiments [14], what could help clarifying the question, whether the mixed quark-hadron phase [7, 8, 15, 16] or the predicted chiral quarkyonic phase [17, 18, 19, 16] can be formed in this energy range.

First theoretical predictions in this energy region were made very recently [14] and they indicate a very rich picture of the physical phenomena in ANC to be investigated, e.g. the formation of high density Mach shock waves and their impact on the spatial distribution of the produced particles and heavier clusters. The main purpose of this work is to formulate the most promising physical issues for the ANC of the BMN program at JINR and to work out the strategy of their experimental exploration.

This work is organized as follows. In the next section we discuss the difference of the directed, elliptic, and triangular flows obtained in ANC and in symmetric nuclear collisions. The third section is devoted to the analysis of the directed, elliptic and triangular flows that may develop, if high density fluctuations occur inside the target nucleus. The last section contains our conclusions.

**2. The unusual properties of ANC.** ANC have some history since they were suggested long ago (see, for instance, [11, 20, 21, 22, 23]), but in those days the analysis of Fourier coefficients of the azimuthal particle distributions was not even suggested. Since the experiments on collisions of identical nuclei is simpler, ANC were forgotten for awhile. After the first work [6] on the analysis of the Fourier coefficients  $v_1, v_2, \dots$  was published this method has become a powerful tool for experimental studies of the evolution process of symmetric heavy ion collisions at high energies [24, 25, 26, 27, 28], i.e. of two identical nuclei ( $A + A$ ). Thus, the quark scaling of the  $v_2$  dependence on the transverse momentum  $p_T$  [28] clearly demonstrated the partonic source of elliptic flow of hadrons at RHIC energies, while the triangular flow is reflecting the correlations that appear at the early stage of collisions [29].

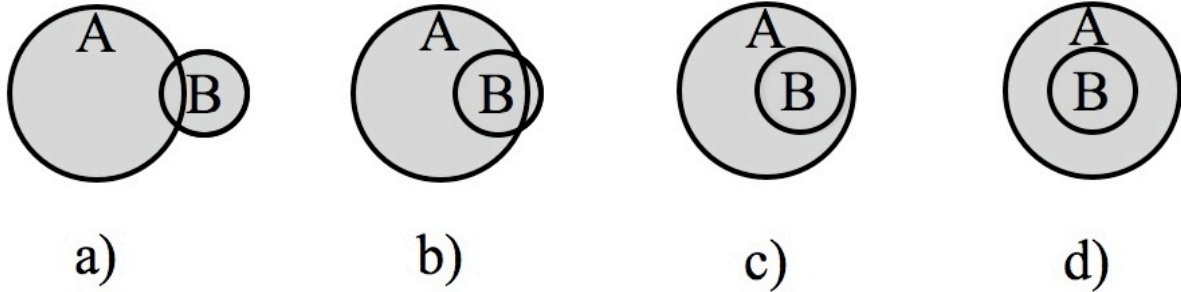


**Fig. 1.** Schematic picture of an asymmetric nuclear collision of nuclei A (large circle) with B (small circle) shown in the transverse plane. The common area of two nuclei is shown for very peripheral collisions (panel a)), for semi-peripheral collisions (panels b) and c)) and for the most central collision (panel d)). Clearly, for semi-peripheral collisions the effect of the shadowing of particle motion to the right hand side of the nucleus B is very weak.

A principally new element of the ANC compared to symmetric nuclear collisions is the generation of strong and asymmetric gradients of energy density and baryonic density at the initial stage of the collision process along with the stronger flow from the target in the direction of the projectile nucleus for a specific choice of the impact parameter values. In contrast to symmetric collisions, in ANC the reflection symmetry between the left nucleus A and the right nucleus B (see panels a)-c) in Fig. 1) is broken from the very beginning. This leads to an entirely different shape and location of the overlap region between the colliding nuclei which, in its turn, results in different flow patterns compared to symmetric  $A + A$  collisions. Indeed, if the impact parameter value is close to  $b_{ANC} \approx 1.1 \text{ fm} \cdot (A^{\frac{1}{3}} - B^{\frac{1}{3}}) \pm 1 \text{ fm}$  (see the panels b) and c) of Fig. 1) and if the size of the target nucleus is chosen close to  $B^{\frac{1}{3}} \approx \frac{1}{2}A^{\frac{1}{3}}$ , then there is sufficient room to vary the impact parameter in the experiment and to select values which are close to  $b_{ANC}$  using an event-by-event analysis. In this case ANC allow us to scan the interior of the target nucleus, as well as to study in detail the variety of surface phenomena such as the surface formation of light nuclear fragments like deuterons, tritons, and heliums nuclei, the emission of high  $p_T$  pions [30], the isospin dependence of hadron surface emission, conical emission due to Mach shock wave formation in the target [14], and so on.

Consider the change in the directed flow first. Although the approximate dependence of the so-called flow parameter  $F$  [31] on  $A^{\frac{1}{3}} + B^{\frac{1}{3}}$ , i.e. on the collision time, was found in the symmetric nuclear collision experiments [32], however, a similar dependence of the directed flow in the ANC is much less certain [26] and has to be studied. In addition, in symmetric nuclear collisions with a lab. energy between 1 and 10 AGeV the effect of nuclear shadowing plays an important role and causes the negative value of pionic  $v_1$  [25]. Since both the peripheral and the most central ANC (see panels a) and d) of Fig. 1) are very similar to the corresponding symmetric nuclear collisions due to a similar geometry, one can expect a similar behavior of their  $v_1$  coefficients, i.e.  $v_1^{AS} \approx v_1^S$ , while for the semi-peripheral ANC (see panels b) and c) in Fig. 1) one expects a different situation. This expectation is supported by the experimental analysis of [12] of pionic flow directed to the in-plane  $OX$ -axis and the one directed oppositely. Therefore, the semi-peripheral ANC would allow one to essentially reduce the effect of shadowing on one side of the formed fireball what could help to finally clarify the source of the strong antiflow of pions [30, 33] with  $p_T < 500 \text{ MeV}$  observed at SIS energies [34] and predicted earlier [35, 36]. Moreover, one can hope to study a rich structure of shock waves in hadronic matter (from conical emission to viscosity) occurring

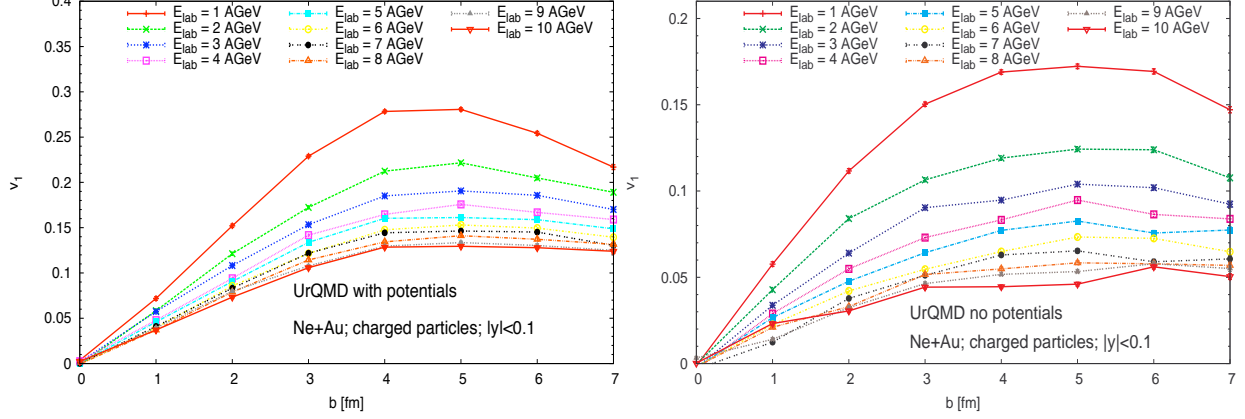


**Fig. 2.** Energy and centrality dependence of the  $v_1^{AS}$  coefficient of charged particles from Ne+Au collisions as calculated with the UrQMD model with potentials (left panel) and without them (right panel). For more details see the text.

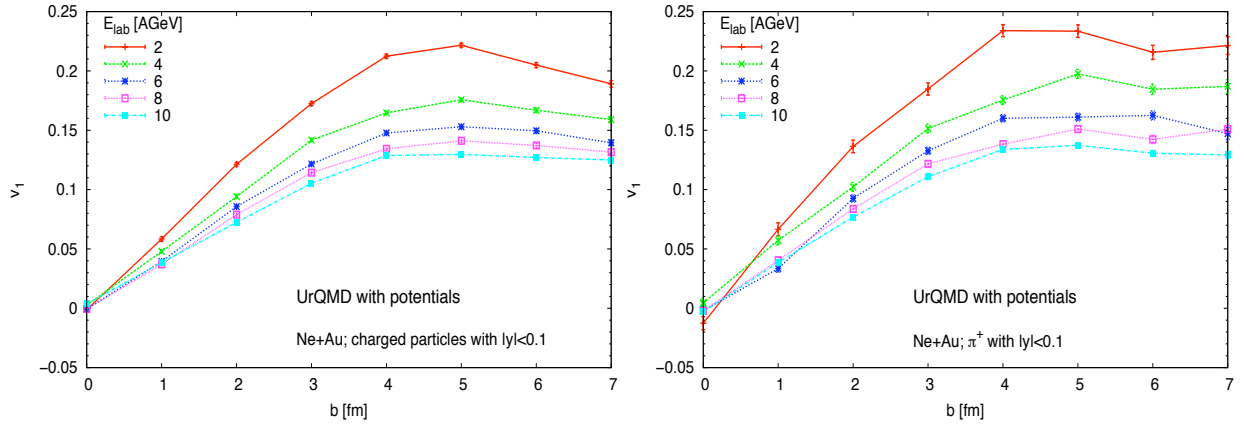


**Fig. 3.** Energy and centrality dependence of the  $v_1^{AS}$  coefficient found by the UrQMD model with potentials for all charged particles (left panel) and for positive pions (right panel) for the ANC Ne+Au.

during semi-peripheral ANC [14].

In order to demonstrate the new possibilities of the ANC we performed the analysis of  $v_1^{AS}$  using the UrQMD model. This model is one of the most successful transport models and was supplemented by in-medium potentials [37, 38, 39] in order to reproduce the full complexity of the flow patterns in the low energy range. For this work, we use the UrQMD model developed in [9, 10, 37, 38, 39] which was thoroughly tested on the available data in a wide range of collision energies. Fig. 2 shows the energy and centrality dependence of the  $v_1^{AS}$  coefficient for all charged particles from the ANC Ne+Au at longitudinal midrapidity in the equal velocity frame of the colliding nuclei. Such a system is convenient to compare the results with both the data obtained in symmetric nuclear collisions and with UrQMD simulations reported earlier [39]. As one can see from Fig. 2 the  $v_1^{AS}$  coefficient of charged particles is essentially non-zero at  $|y| < 0.1$  for ANC, whereas it is zero for  $y = 0$  in symmetric nuclear collision since it is an odd function of the center of mass rapidity. Also Fig. 2 demonstrates that inclusion of the potentials in the UrQMD model [37, 38, 39] is important since their absence leads to roughly double decrease of the directed flow coefficient. A comparison of the charged particles directed flow with that one of positive pions shows a complete similarity in the energy and centrality dependence (see Fig. 3). The behavior of negative pions is also similar. Figs. 2 and 3 demonstrate a gradual decrease of the directed flow (left-right asymmetry) with the increase of the collision energy.

Let us now consider the qualitative change of the elliptic flow (in-plane) coefficient behavior in ANC. The experimental data show that at lab. energies of about 3.3 AGeV the

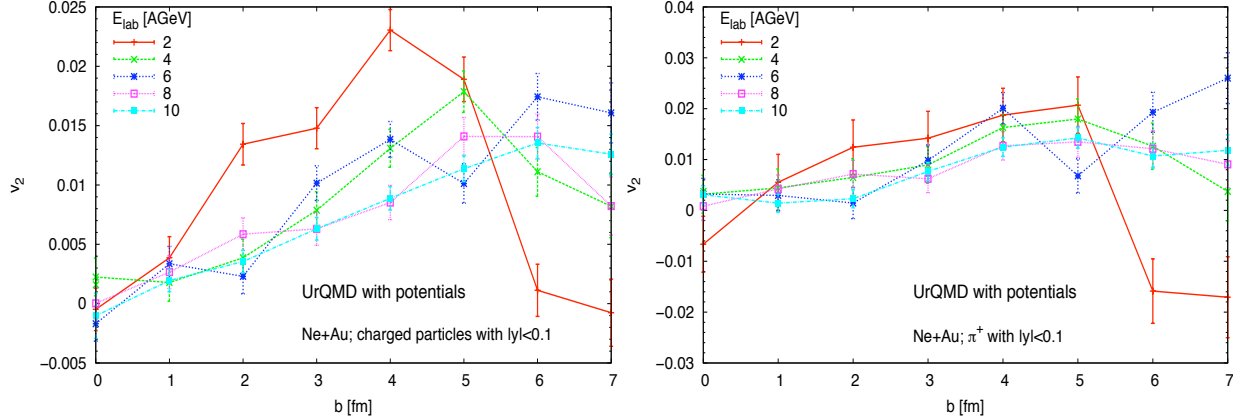


**Fig. 4.** Energy and centrality dependence of the  $v_2^{AS}$  coefficient found by the UrQMD model with potentials for charged particles (left panel) and for positive pions (right panel) in the ANC Ne+Au.

elliptic flow in symmetric collisions is zero, i.e.  $v_2^S = 0$ , and its value slowly grows with the colliding energy [27]. The reason for those small values of the elliptic flow around this energy is that the slow moving remnants of the target (projectile) nucleus  $A$  ( $B$ ) shadow the motion of particles from the collision zone directed from nucleus  $A$  to nucleus  $B$  (see Fig. 1). The change of the  $v_2^S$  sign at 3.3 AGeV signifies the transition from the out-of-plane to the in-plane elliptic flow which was predicted long ago [40].

Due to a similar geometry both the peripheral and the most central ANC are alike the corresponding symmetric nuclear collisions, and therefore, in this case one has to expect almost identical behavior of their  $v_2$  coefficients, i.e.  $v_2^{AS} \approx v_2^S$ . On the other hand, the semi-peripheral collisions (panels b) and c) in Fig. 1) produce an entirely different situation: in this case, if the smaller nucleus  $B$  hits the larger nucleus  $A$  at its boundary, not too far above or below its surface, i.e. for impact parameter values close to  $b_{ANC}$ , then the whole situation concerning the shadowing is changed. At these impact parameter values there is almost no shadowing on one side and, hence, one can expect that in those ANC the  $v_2^{AS}$  coefficient can essentially be enhanced at lab. energies between 2 and 5 AGeV. In addition, one can expect that some number of slow moving particles with an initial momentum directed from nucleus  $B$  to nucleus  $A$  is reflected backwards and creates an additional flow in the direction of the no-shadowing side of the collision region leading to positive values of  $v_2^{AS}$ . These new features of the ANC elliptic flow can be seen in Fig. 4. For  $E_{lab} = 2$  AGeV both the charged particles and pions have positive  $v_2^{AS}$  coefficient for semi-peripheral collisions, while for central and peripheral collisions the pionic  $v_2^{AS}$  is negative. As the collision energy is increased, the maximum of the  $v_2^{AS}$  coefficient gradually moves to larger impact parameter values and gets less pronounced.

In this work we report the first simulations of the triangular flow coefficient for the low collision energy range. Recent analyses [29, 1, 2, 3, 4, 5, 41] clearly demonstrated an importance of the  $v_3$  coefficient for an elucidation of the experimental information and here we confirm this fact. Although the  $v_3^{AS}$  signal found for  $E_{lab} = 2 - 10$  AGeV is much weaker than that one determined at RHIC energies, the structure of triangular flow at low collision energies is definitely much richer as one can see from Fig. 5. Indeed, for  $E_{lab} = 2 - 3$  AGeV the charge particles (negative pions) predict that the  $v_3^{AS}$  coefficient has a maximum in semi-peripheral collisions whereas  $v_3^{AS}$  is negative at impact parameter values of  $b \approx 1$  fm ( $b < 1$  fm) and  $b \geq 6$  fm. For  $E_{lab} = 4 - 5$  AGeV the maximum of the  $v_3^{AS}$  coefficient is still clearly seen, although it gets wider, whereas for larger collision energies this maximum is not that clearly visible especially for pions (see the right panel in Fig. 5).

**3. The dense spot effect on flow patterns.** The existence of high density fluctuations in ordinary nuclei is debated for a long time [42, 43] along with their possible applications in

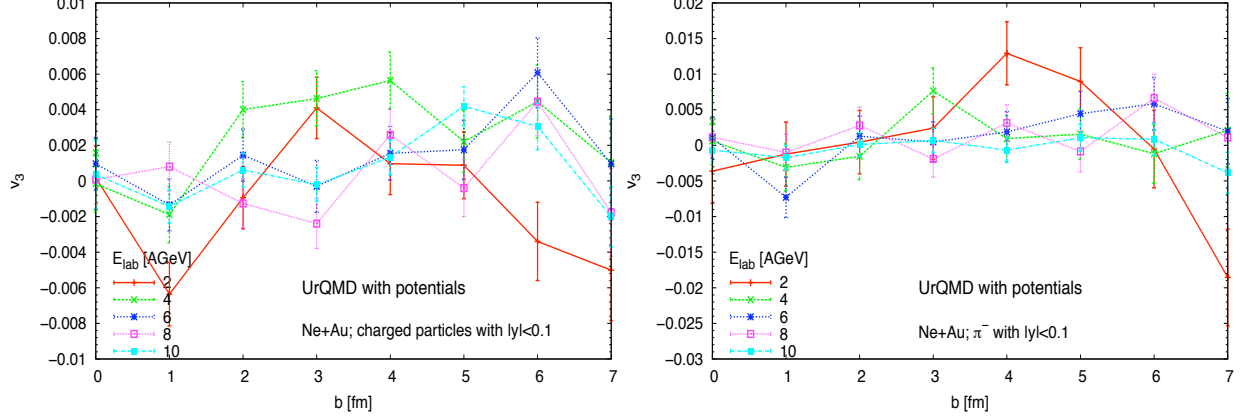


**Fig. 5.** Energy and centrality dependence of the  $v_3^{AS}$  coefficient found by the UrQMD model with potentials for charged particles (left panel) and for negative pions (right panel) in the ANC Ne+Au.

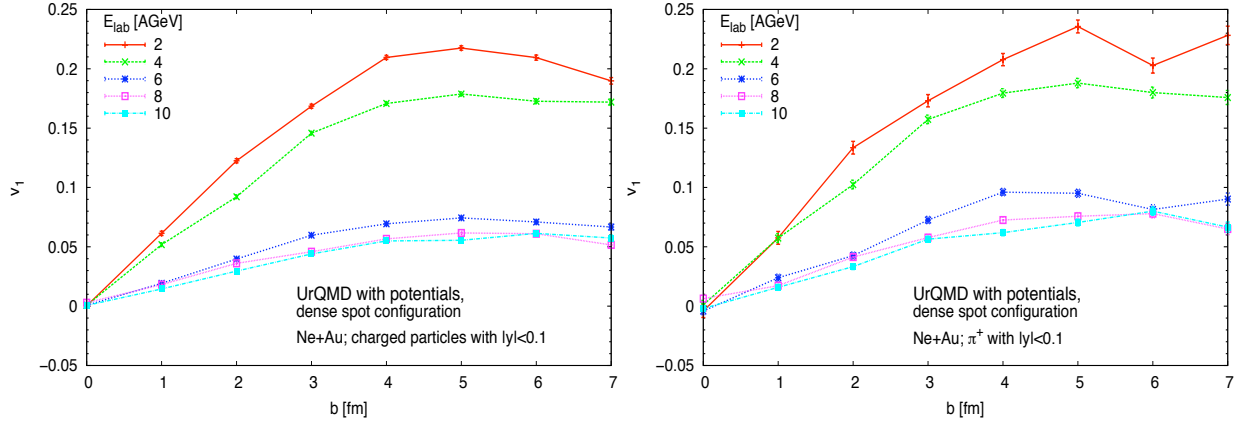


**Fig. 6.** Same as in Fig. 3, but for the dense spot configuration (see text for details).

the context of the heavy ion reactions [44, 45]. Here we would like to recapitulate this issue and to study the influence of the high density fluctuations on the  $v_1^{AS}$ ,  $v_2^{AS}$  and  $v_3^{AS}$  coefficients for ANC. To estimate this effect, we randomly put 20 nucleons from the  $A_3$ -nucleus in a narrow Gaussian distribution inside of the ordinary Monte Carlo sampled nucleus. This gives us a fluctuating dense spot initial configuration for the target nucleus. Such a mild assumption is far from the extremely high densities discussed with respect to flucton [42, 45]. The dense spot is fixed in the center of the Au target with an offset in x-direction of half of the impact parameter between the two colliding nuclei. The condition that there is an overlap between the dense spot of the radius  $1.1 B^{\frac{1}{3}}$  fm and the projectile nucleus of the same radius is  $b - 1.1 B^{\frac{1}{3}} \text{ fm} \leq \frac{b}{2} + 1.1 B^{\frac{1}{3}} \text{ fm}$ . That means, for impact parameters of the Ne+Au reaction of  $b \leq 4.4 B^{\frac{1}{3}} \text{ fm} \approx 12 \text{ fm}$  such an overlap always exists.

The results for the  $v_1^{AS}$ ,  $v_2^{AS}$  and  $v_3^{AS}$  coefficients are presented in Figs. 6–8. Comparing Figs. 3 and 6, one sees that the directed flow for collisions with the target exhibiting the dense spot and for collisions without it have almost an identical centrality dependence for the energies  $E_{\text{lab}} = 2 - 4 \text{ AGeV}$ . However, for  $E_{\text{lab}} \geq 5 \text{ AGeV}$  the  $v_1^{AS}$  coefficient with the dense spot is just 50 % of the  $v_1^{AS}$  coefficient without dense spot. Thus, there is a non-monotonic behavior of the directed flow coefficient with respect to the collision energy. From the analysis of energy density we conclude that it indicates the change of regimes from the dominance of the target break up process at  $E_{\text{lab}} = 2 - 4 \text{ AGeV}$  to a strong compression and more intense thermalization of the reaction zone for  $E_{\text{lab}} \geq 5 \text{ AGeV}$ . Qualitatively a similar picture is valid for the elliptic flow coefficient of the dense spot configuration: for  $E_{\text{lab}} = 2 - 4 \text{ AGeV}$  the  $v_2^{AS}$  coefficients with the dense spot are similar to that ones

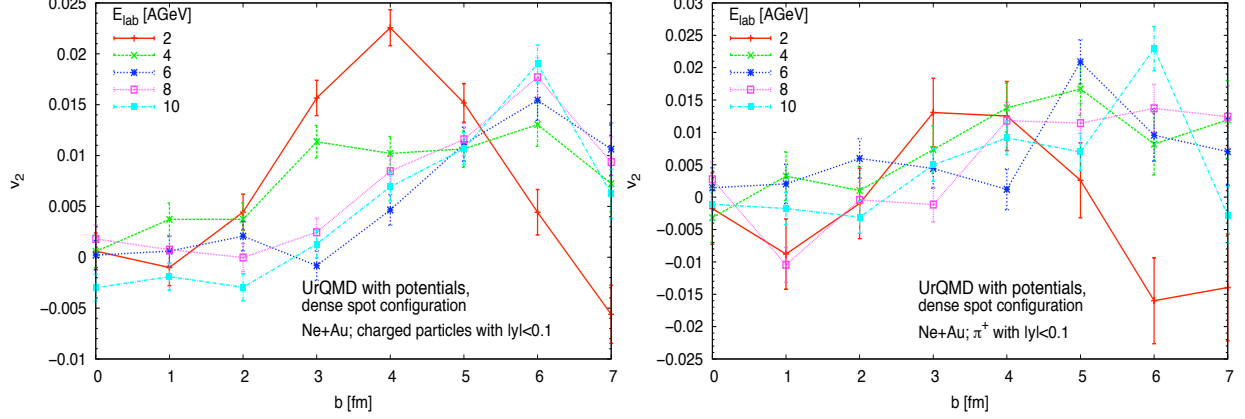


**Fig. 7.** Same as in Fig. 4, but for the dense spot configuration.

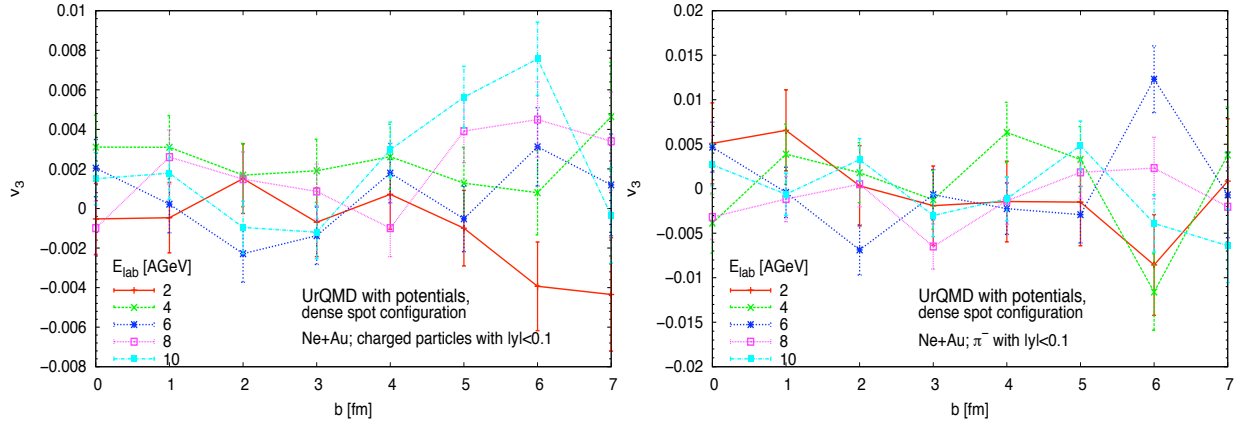


**Fig. 8.** Same as in Fig. 5, but for the dense spot configuration.

without it, whereas for  $E_{\text{lab}} \geq 5$  AGeV the elliptic flow coefficient with the dense spot has different centrality dependence (compare Figs. 4 and 7). The latter means that, in contrast to the case of the dense spot absence, for  $E_{\text{lab}} \geq 5$  AGeV the elliptic flow coefficient of the charged particles is close to zero, i.e.  $v_2^{\text{AS}} \approx 0$ , for  $b \leq 3$  fm while its peak is now located at  $b = 6$  fm. On the other hand, the  $v_2^{\text{AS}}$  coefficient of positive pions exhibits a W-shape for  $E_{\text{lab}} = 2$  AGeV, whereas for  $E_{\text{lab}} \geq 4$  AGeV its centrality dependence is similar to the elliptic flow coefficient of protons and charged particles. Also, one has to admit that for  $E_{\text{lab}} \geq 4$  AGeV the maximal amplitudes of the elliptic flow of both the charged particles, protons and pions for the dense spot configurations (Fig. 7) are not reduced in strength compared to the ANC without dense spot (Fig. 4). Thus, the 50 % reduction of the directed flow for the dense spot configurations at  $E_{\text{lab}} \geq 4$  does not lead to a dramatic change of the corresponding elliptic flow at these energies.

Again the essential change in the centrality dependence of the  $v_3^{\text{AS}}$  coefficient for the dense spot configuration is seen at  $E_{\text{lab}} \leq 4$  AGeV (see Fig. 8): the clear maximum located at about  $b = 3 - 4$  fm for the no dense spot case (see Fig. 5) disappears in the dense spot configurations. Only for energies  $E_{\text{lab}} \geq 8$  AGeV one can see some increase of the maximal value of  $v_3^{\text{AS}}$  coefficient compared to the no dense spot case.

**4. Conclusions.** Using the UrQMD model including potentials [37, 38, 39] here we perform a comprehensive analysis of the directed, elliptic and triangular flow coefficients for asymmetric nuclear collisions (ANC) for the first time and suggest to explore this promising aspect of heavy ion physics in the energy range of the BMN program at JINR and the FAIR heavy ion program. We argue that a specific choice of the impact parameter should lead to the disappearance of the nuclear shadowing effect on the side of smaller colliding nucleus and show that such an effect leads to an essential enhancement of the directed and elliptic flows



of hadrons in ANC compared to the symmetric nuclear collisions.

Our analysis shows that the centrality and energy dependencies of the  $v_1^{AS}$ ,  $v_2^{AS}$  and  $v_3^{AS}$  coefficients found for ANC are richer and more complicated compared to symmetric nuclear collisions. Furthermore, we find that these flow patterns are very sensitive to the details of the employed interaction which can be used both for fine tuning of transport codes and for elucidation of the essential features of the hadron interaction in the medium.

Also, we demonstrate that the possible existence of high density fluctuations in the large target nucleus may be verified using ANC, since they allow one to scan the target interior by a smaller projectile and to draw physical conclusions from the centrality and the energy dependencies of directed, elliptic and triangular flows on an event-by-event basis. The found non-monotonic energy dependence of the directed flow indicates a higher degree of compression reached in ANC with the dense spot configuration at lab. energies above 5 AGeV.

All these new results allow us to hope that the low energy ANC will soon become a powerful tool of theoretical and experimental studies of the strongly interacting matter properties.

**Acknowledgments.** The authors are thankful to S. Voloshin for many fruitful discussions. K.A.B. acknowledges the partial support of the Program 'Fundamental Properties of Physical Systems under Extreme Conditions' launched by the Section of Physics and Astronomy of National Academy of Sciences of Ukraine. The work of A.S.S. was supported in part by the Russian Foundation for Basic Research, Grant No. 11-02-01538-a. The work of P.R. and J.S. was supported by BMBF, HGS-HIRe, and the Hessian LOEWE initiative through the Helmholtz International Center for FAIR. All computational resources were provided by the Frankfurt LOEWE Center for Scientific Computing (LOEWE-CSC).

## References

- [1] S. Bathe for the PHENIX Collaboration, Plenary talk at the conference "Quark Matter 2011", Annecy, France, May 23-28, 2010.
- [2] H. Masui for the STAR Collaboration, Plenary talk at the conference "Quark Matter 2011", Annecy, France, May 23-28, 2010.
- [3] J. Schukraft for the ALICE Collaboration, Plenary talk at the conference "Quark Matter 2011", Annecy, France, May 23-28, 2010.
- [4] P. Steinberg for the ATLAS Collaboration, Plenary talk at the conference "Quark Matter 2011", Annecy, France, May 23-28, 2010.
- [5] B. Wyslouch for the CMS Collaboration, Plenary talk at the conference "Quark Matter 2011", Annecy, France, May 23-28, 2010.
- [6] S. Voloshin and Y. Zhang, *Z. Phys. C* **70**, 665 (1996).
- [7] A.N. Sissakian, A.S. Sorin, M.K. Suleymanov, V.D. Toneev and G.M. Zinovjev, *Phys. Part. Nucl. Lett.* **5**, (2008) 1.
- [8] NICA White Paper v.3.3, Chapter I, <http://theor.jinr.ru/twiki/pub/NICA/WebHome/> and references therein.
- [9] S. A. Bass *et al.*, *Prog. Part. Nucl. Phys.* **41**, 255 (1998).
- [10] M. Bleicher *et al.*, *J. Phys. G* **25** (1999) 1859.
- [11] H. G. Baumgardt *et al.*, *Z. Phys.* **A273** (1975) 359-371.
- [12] J. Gosset *et al.*, *Phys. Rev. Lett.* **62**, (1989) 1251.
- [13] B. Adyasevich *et al.*, *Nucl. Phys. B (Proc. Suppl.)* **16**, (1990) 419c.
- [14] P. Rau, J. Steinheimer, B. Betz, H. Petersen, M. Bleicher and H. Stöcker, [arXiv:1003.1232](https://arxiv.org/abs/1003.1232) [nucl-th].



- [15] J. Randrup, NICA White Paper v.3.3, [http://theor.jinr.ru/twiki/pub/ NICA/ Web-Home/](http://theor.jinr.ru/twiki/pub/NICA/WebHome/)
- [16] for a discussion and estimates see D. Blaschke, F. Sandin, V. Skokov and S. Typel, NICA White Paper v.3.3, [http://theor.jinr.ru/twiki/pub/ NICA/WebHome/](http://theor.jinr.ru/twiki/pub/NICA/WebHome/) and refences therein.
- [17] L. McLerran and R. D. Pisarski, Nucl. Phys. A **796**, (2007) 83.
- [18] Y. Hidaka, L. D. McLerran, and R. D. Pisarski, Nucl. Phys. A **808**, (2008) 117; L. McLerran, K. Redlich, and C. Sasaki, Phys. A **824**, (2009) 86; K. Fukushima, Phys. Rev. D **77**, (2008) 114028; L. Y. Glozman and R. F. Wagenbrunn, Phys. Rev. D **77**, (2008) 054027.
- [19] A. Andronic et al., arXiv:0911.4806v3 [hep-ph] and references therein.
- [20] J. Hofmann, H. Stoecker, U. W. Heinz, W. Scheid, W. Greiner, Phys. Rev. Lett. **36** (1976) 88-91.
- [21] H. Stöcker, J. A. Maruhn and W. Greiner, Z. Phys. A **293**, (1979) 173.
- [22] H. Stöcker, J. A. Maruhn and W. Greiner, Phys. Rev. Lett. **44**, (1980) 725.
- [23] H. Stöcker, C. Riedel, Y. Yariv, L. P. Csernai, G. Buchwald, G. Graebner, J. A. Maruhn, W. Greiner *et al.*, Phys. Rev. Lett. **47** (1981) 1807-1810.
- [24] W. Reisdorf and H. G. Ritter, Ann. Rev. Nucl. Part. Sci. **47**, (1997) 663.
- [25] J. Y. Ollitrault, Nucl. Phys. A **638**, (1998) 195 and references therein.
- [26] N. Herrmann, J. P. Wessels and Th. Wienold, Ann. Rev. Nucl. Part. Sci. **49**, (1999) 581.
- [27] see R. Stock, J. Phys.G **30**, (2004) S633 and references therein.
- [28] S. S. Adler et al. (PHENIX Collaboration), Phys. Rev. Lett. **91**, (2003) 182301; J. Adams et al. (STAR Collaboration), Phys. Rev. Lett. **95**, (2005) 122301; A. Adare et al. (PHENIX Collaboration), Phys. Rev. Lett. **98**, (2007) 162301.
- [29] B. Alver and G. Roland, Phys. Rev. C **81**, (2010) 054905.
- [30] for a discussion see E. E. Zabrodin, C. Fuchs, L. V. Bravina and A. Faessler, Phys. Rev. C **63**, (2001) 034902.
- [31] K. G. R. Doss et al., Phys. Rev. Lett. **57**, (1986) 302.
- [32] Ph. Crochet et al., FOPI Collaboration, Nucl. Phys. A **627**, (1997) 522.
- [33] H. Stöcker, Nucl. Phys. **A750** (2005) 121-147.
- [34] A. Wagner et al., Phys. Rev. Lett. **85**, 18 (2000).
- [35] B.-A. Li, W. Bauer, and G. F. Bertsch, Phys. Rev. C **44**, 450 (1991).
- [36] S. A. Bass, C. Hartnack, H. Stöcker, and W. Greiner, Phys. Rev. Lett. **71**, 1144 (1993); Phys. Rev. C **50**, 2167 (1994).
- [37] Q. -f. Li, Z. -x. Li, S. Soff, M. Bleicher, H. Stoecker, J. Phys. G **G32** (2006) 151-164.
- [38] Q. -f. Li, Z. -x. Li, S. Soff, M. Bleicher, H. Stoecker, J. Phys. G **G32** (2006) 407-416.
- [39] H. Petersen, Q. Li, X. Zhu and M. Bleicher, Phys. Rev. C **74**, 064908 (2006).
- [40] J.-Y. Ollitrault, Phys. Rev. D **46**, (1992) 229.
- [41] H. Petersen, G.-Y. Qin, S. A. Bass and B. Müller, arXiv:1008.0625v2 [nucl-th].
- [42] D. I. Blokhintsev, ZhETP **6**, (1958) 995.
- [43] A. Bohr and B. Mottelson, "Nuclear Structure", Benjamin Press, New York, 1975, Vol.2.
- [44] D. Seibert, Phys. Rev. Lett. **63**, (1989) 136.
- [45] A. Stavinskiy et al., NICA White Paper v.3.3, [http://theor.jinr.ru/twiki/pub/ NICA/WebHome/](http://theor.jinr.ru/twiki/pub/NICA/WebHome/) and refences therein.